

## Electronic Supplementary Information

for

A “naked eyes” and ratiometric fluorescent chemosensor for rapid detection of fluoride based on combination of desilylation reaction and excited state proton transfer

Yinyin Bao, Bin Liu, Hu Wang, Jiao Tian and Ruke Bai\*

*CAS Key Laboratory of Soft Matter Chemistry, Department of Polymer Science and Engineering, University of Science and Technology of China, Hefei, P. R. China 230026.*

*E-mail: [bairk@ustc.edu.cn](mailto:bairk@ustc.edu.cn)*

*Tel: 0086-551-3600722; Fax: 0086-551-3631760*

### Contents

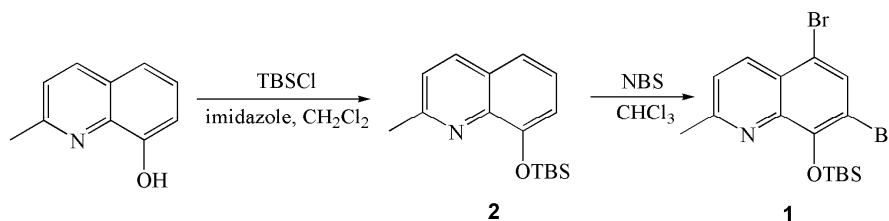
1. Materials and Methods.
2. Synthesis and Characterization.
3. UV-visible Absorbance Analysis.
4. Fluorometric Analysis.
5.  $^1\text{H}$  NMR Analysis
6. NMR and MS Data.

## 1. Materials and Methods.

Anionic compounds such as  $[\text{Bu}_4\text{N}]^+\text{Cl}^-$ ,  $[\text{Bu}_4\text{N}]^+\text{Br}^-$ ,  $[\text{Bu}_4\text{N}]^+\text{ClO}_4^-$ ,  $[\text{Bu}_4\text{N}]^+\text{HSO}_4^-$ ,  $\text{NaNO}_3$ ,  $\text{NaOAc}$  and  $\text{NaH}_2\text{PO}_4$  were purchased from Shanghai Chemical Co.,  $[\text{Bu}_4\text{N}]^+\text{F}^-$  was purchased from J&K Chemical Co. and 2-methyl-8-hydroxyquinoline was a Alfa Aesar Co. product. They were used without further purification.  $\text{CH}_2\text{Cl}_2$  was purchased from Shanghai Chemical Co. and dried over anhydrous  $\text{Na}_2\text{SO}_4$ . 8-*tert*-butyldimethylsilyloxy-2-methylquinoline<sup>1</sup> was prepared according to the literature. All the other reagents were purchased and used without further purification.

Fluorescence spectra measurements were performed on a Shimadzu RF-5301PC spectrofluorophotometer. Absorption spectra were determined on a Pgeneral UV-Vis TU-1901 Spectrophotometer. <sup>1</sup>H and <sup>13</sup>C NMR spectra were taken on a Bruker AVANCE II spectrometer with TMS as an internal standard and  $\text{CDCl}_3$  or  $\text{DMSO-d}_6$  as solvent. MS were performed on a ProteomeX-LTQ spectrometer. All spectra were recorded at room temperature (temperature controlled at  $25 \pm 3$  °C).

## 2. Synthesis and characterization.



### 5,7-Dibromo-8-*tert*-butyldimethylsilyloxy-2-methylquinoline(**1**)

To a round-bottom flask were added a solution of 8-*tert*-butyldimethylsilyloxy-2-methylquinoline(**2**) (1.27 g, 4.65 mmol) and NBS (1.65 g, 9.30 mmol) in  $\text{CHCl}_3$  (15 ml). The solution was stirred overnight at room temperature. Then it was poured into distilled water (40 ml), and the resulting mixture was extracted three times with  $\text{CH}_2\text{Cl}_2$ . The combined organic layer was dried over anhydrous  $\text{Na}_2\text{SO}_4$ , and concentrated under vacuum. Compound (**1**) was isolated using a silica gel chromatographic column eluted with petroleum ether/ethyl acetate (v/v, 12:1), resulting a light yellow solid in 53% yield. <sup>1</sup>H NMR (400 MHz,  $\text{CDCl}_3$ ):  $\delta$  = 8.29(d, 1H,  $J$ =8.8Hz), 7.86(s, 1H), 7.34(d, 1H,  $J$ =8.8Hz), 2.75(s, 3H), 1.10(s, 9H), 0.38(s, 6H). <sup>13</sup>C NMR (100 MHz,  $\text{CDCl}_3$ ):  $\delta$  = 158.1, 150.1, 141.3, 135.8, 133.1, 126.1, 123.4, 112.3, 111.5, 26.3, 24.3, 19.7, -2.5. MS:  $m/z$ : Calcd: 429.9759  $[\text{M}+\text{H}]^+$ , Found: 429.96  $[\text{M}+\text{H}]^+$ .

### 3. UV-visible Absorbance Analysis.

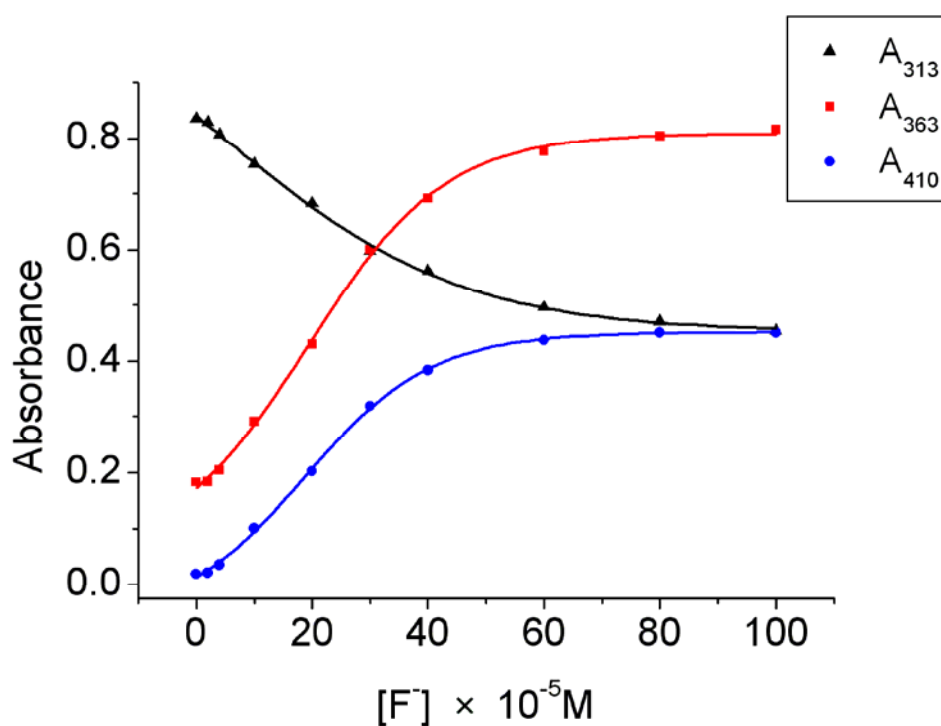


**Fig. S1.** UV-vis absorbance changes of sensor **1** vs TBAF concentration at 313, 363 and 410 nm.  $[1] = 200 \mu M$ .

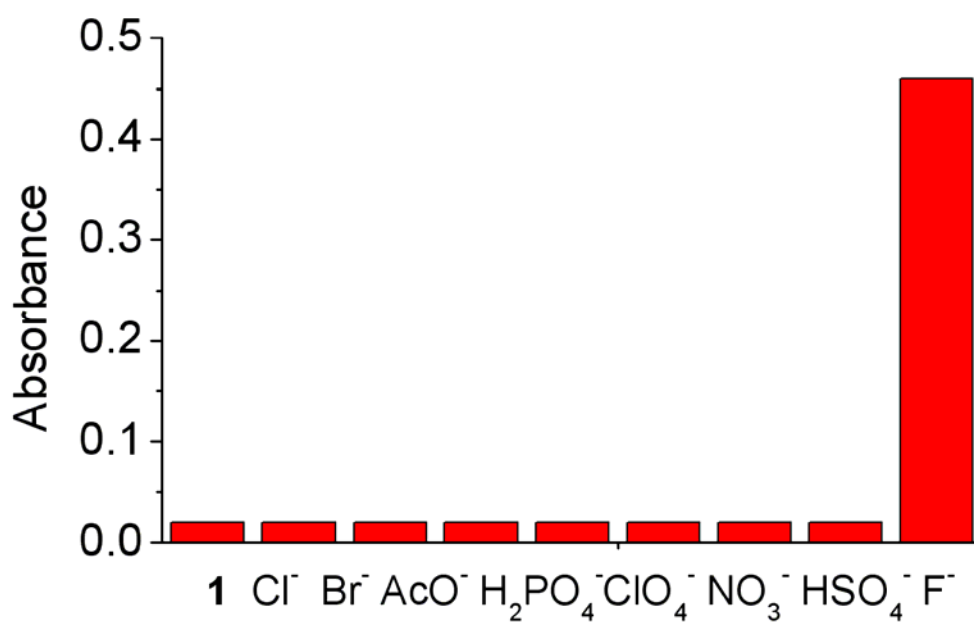


**Fig. S2.** UV-vis absorbance of the sensor **1** at 410 nm in the presence of 10 equivalents of different anions in THF.  $[1] = 200 \mu M$ .

#### 4. Fluorometric Analysis.

The quantum yields of sensor **1** in different solvents were determined according to the following equation:

$$\Phi_u = \Phi_s \frac{F_u A_s n_u^2}{F_s A_u n_s^2}$$

Where  $\Phi$  is quantum yield;  $F$  is integrated area under the corrected emission spectra;  $A$  is absorbance at the excitation wavelength;  $n$  is the refractive index of the solution; the subscripts  $u$  and  $s$  refer to the unknown and the standard, respectively. Quinine bisulfate in 0.05 M H<sub>2</sub>SO<sub>4</sub> solution was used as the standard, which has a quantum yield of 0.55.

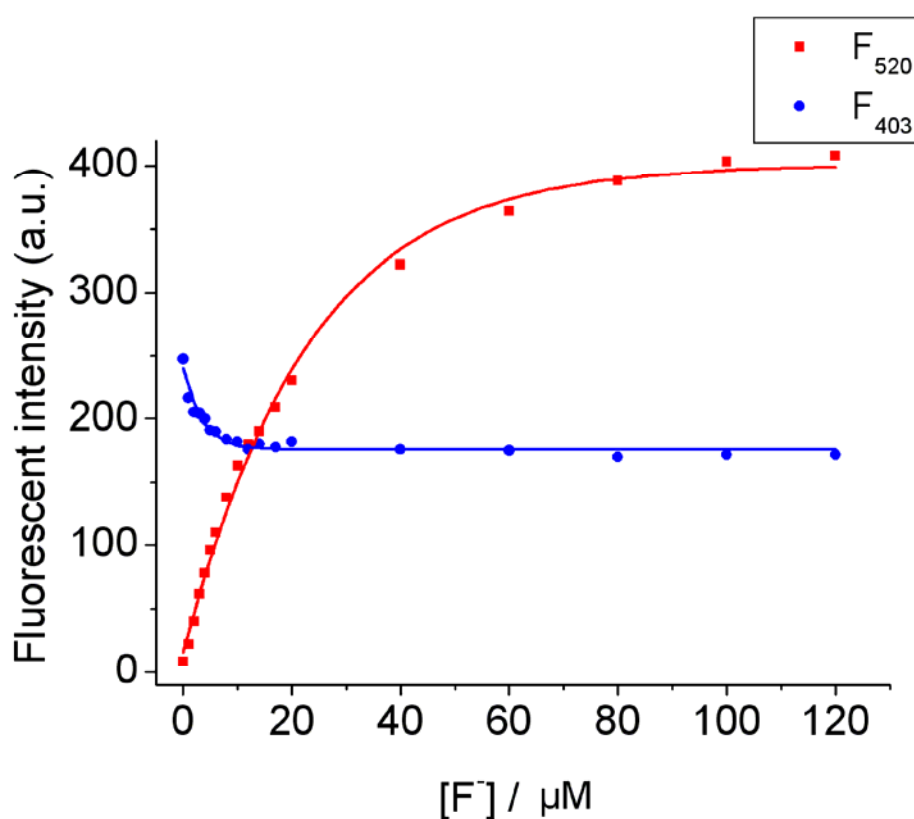


**Fig. S3.** Fluorescence emission changes of sensor **1** vs TBAF concentration at 403 and 520 nm in THF. [1] = 20 μM.  $\lambda_{\text{ex}} = 338$  nm.

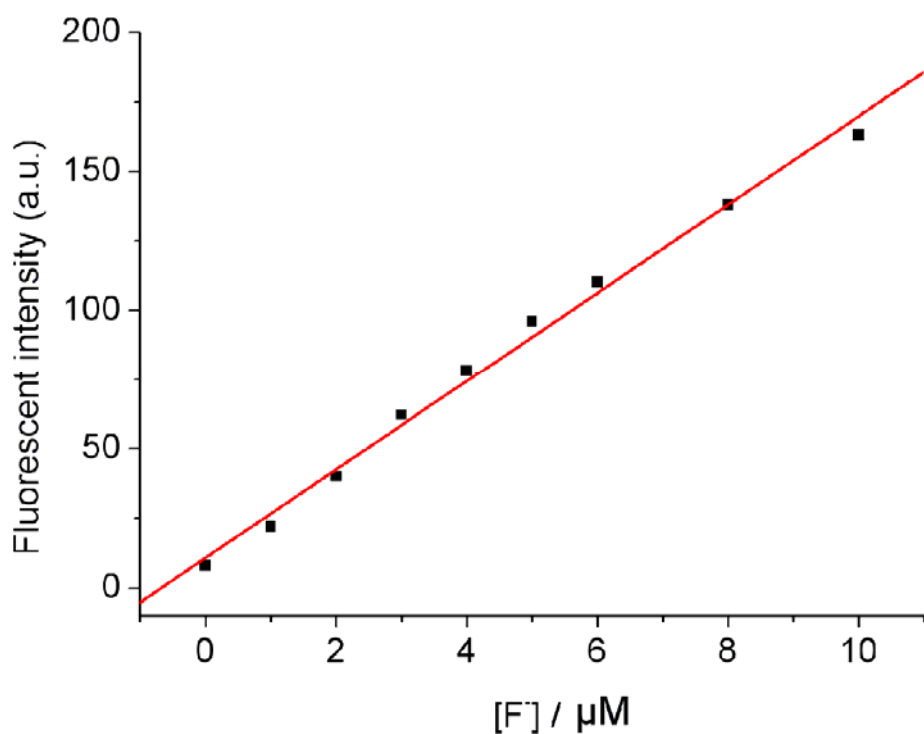


**Fig. S4.** Fluorescence emission changes of sensor **1** at 520 nm vs TBAF concentration form 0 to 10  $\mu\text{M}$ .  $[\mathbf{1}] = 20 \mu\text{M}$ .  $\lambda_{\text{ex}} = 338 \text{ nm}$ .

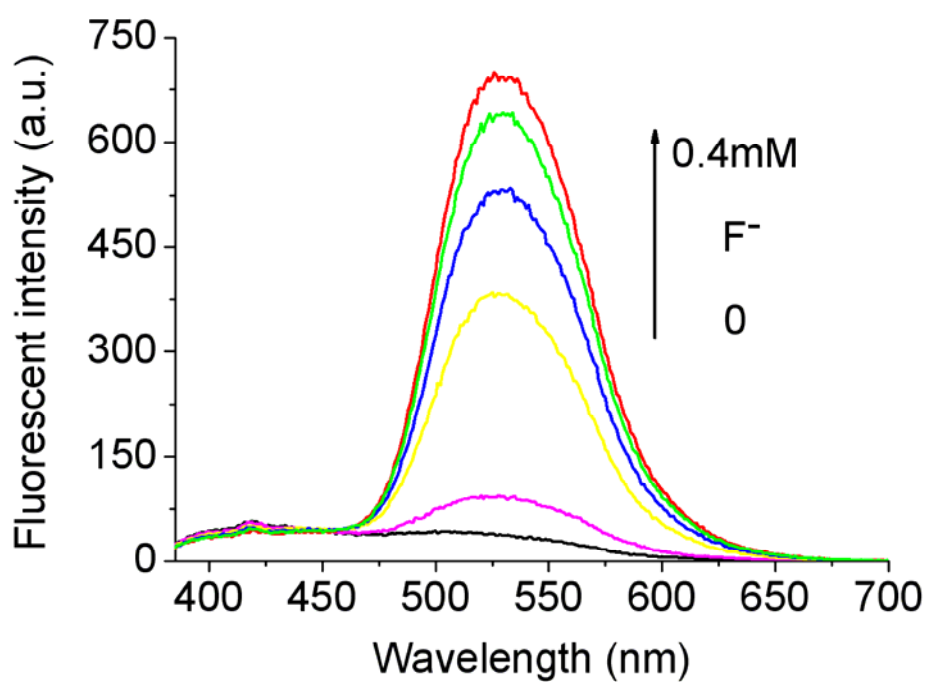


**Fig. S5.** Fluorescence spectra of 5,7-dibromo-8-hydroxyquinoline ( $20\mu\text{M}$ ) + TBAF in THF in the presence of increasing  $\text{F}^-$  concentrations.  $\lambda_{\text{ex}} = 360 \text{ nm}$ .

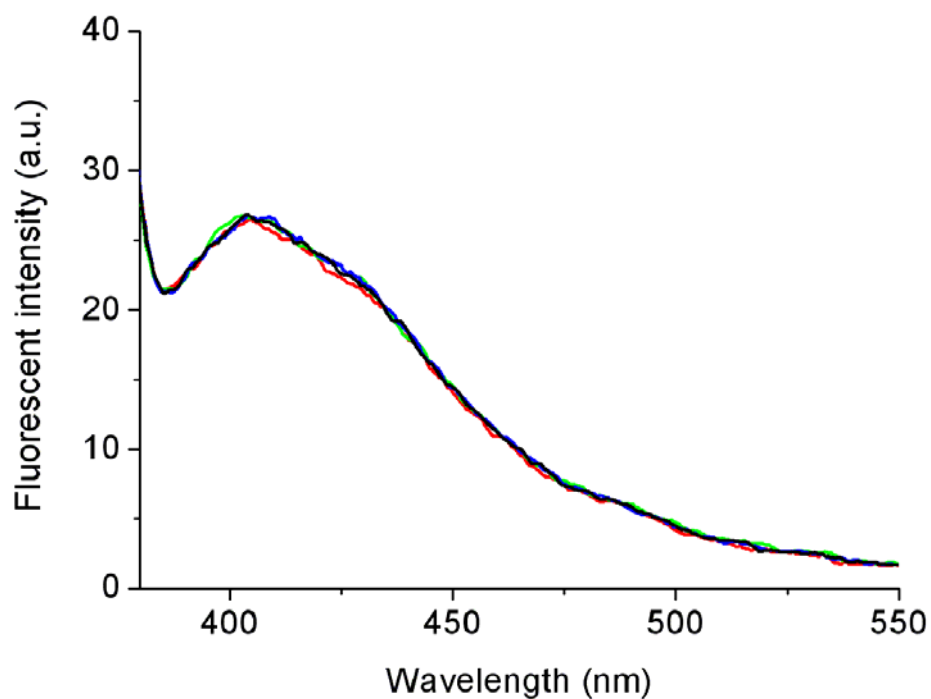


**Fig. S6.** Fluorescence spectra of 8-*tert*-butyldimethylsilyloxy-2-methylquinoline (20  $\mu$ M) + TBAF (0, 0.08 mM, 0.16 mM, 0.4 mM) in THF.  $\lambda_{\text{ex}} = 360$  nm.

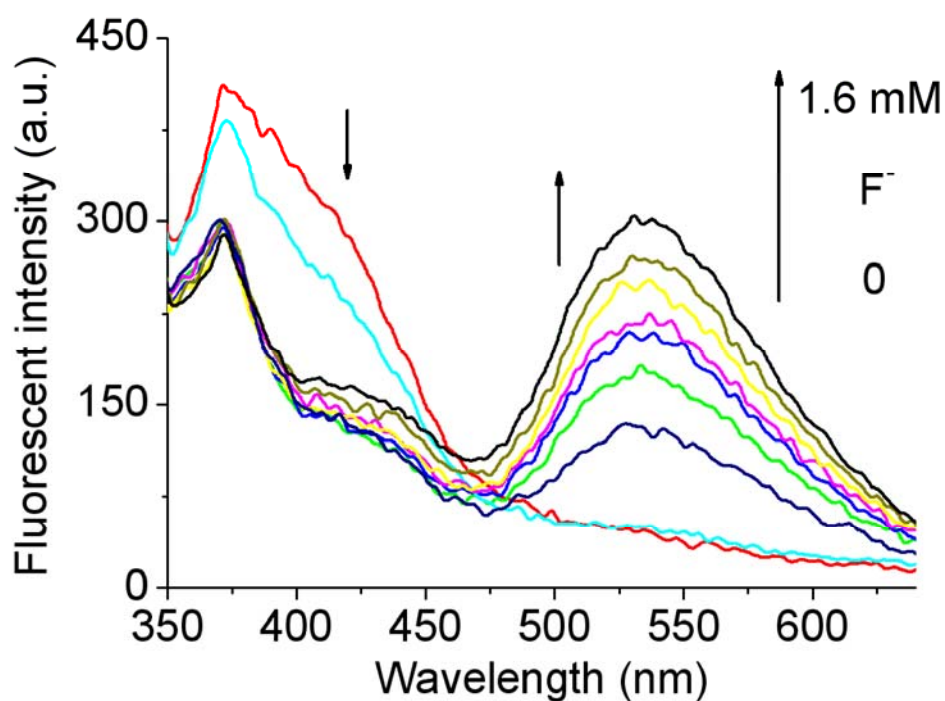


**Fig. S7.** Fluorescence spectra of sensor 1 + TBAF in DMF/H<sub>2</sub>O (95:5, v/v) in the presence of increasing F<sup>-</sup> concentrations. [1] = 20  $\mu$ M.  $\lambda_{\text{ex}} = 335$  nm.

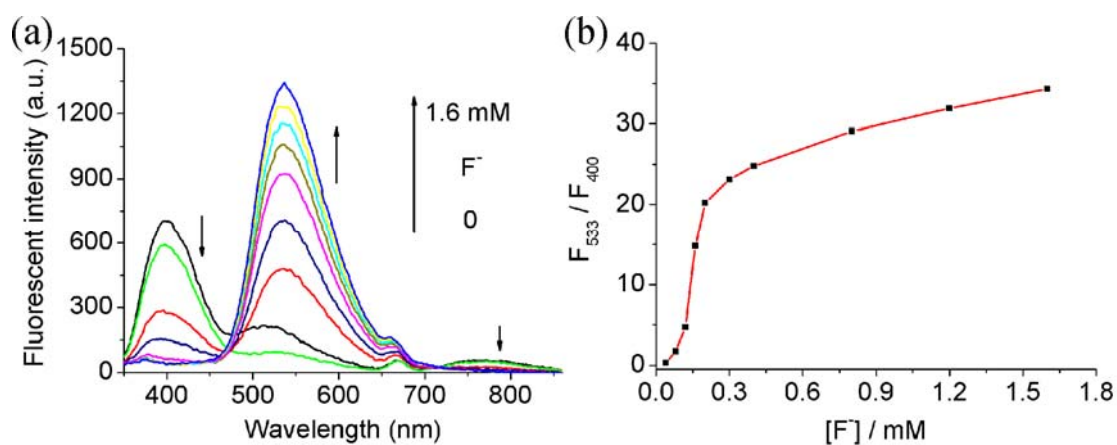


**Fig. S8** (a) Fluorescence spectra of sensor **1** + TBAF in DMF/H<sub>2</sub>O (95:5, v/v) in the presence of increasing  $F^-$  concentrations. (b) Ratiometric calibration curves  $F_{533\text{nm}}/F_{403\text{nm}}$  as a function of  $F^-$  concentrations.  $[1] = 200 \mu\text{M}$ .  $\lambda_{\text{ex}} = 335 \text{ nm}$ .

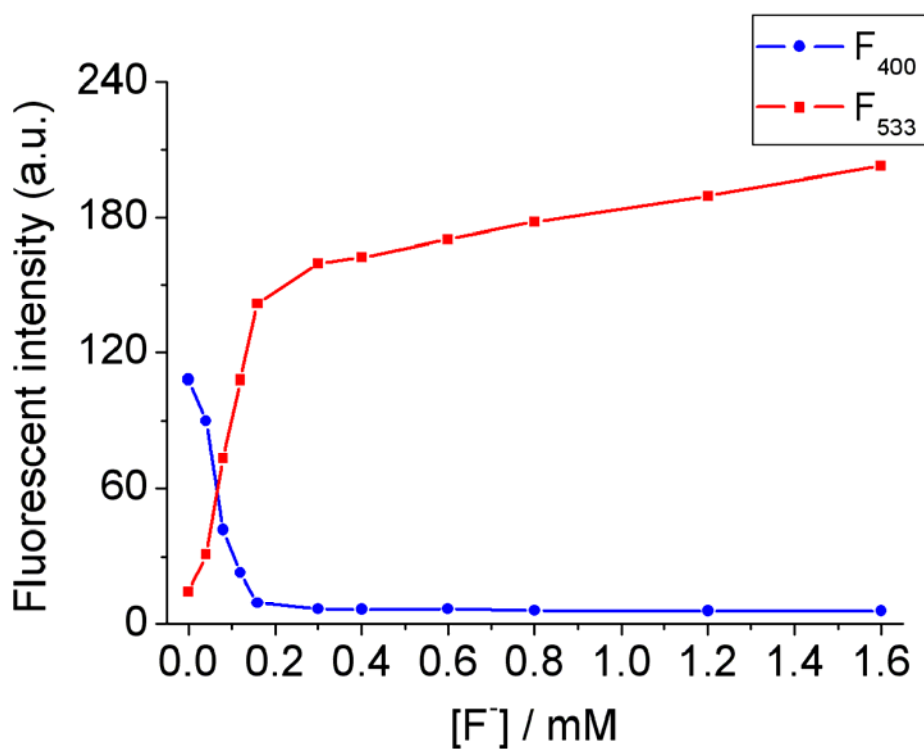


**Fig. S9**. Fluorescence emission changes of sensor **1** vs TBAF concentration at 400 and 533 nm in DMF/H<sub>2</sub>O (95:5, v/v).  $[1] = 200 \mu\text{M}$ .  $\lambda_{\text{ex}} = 335 \text{ nm}$ .

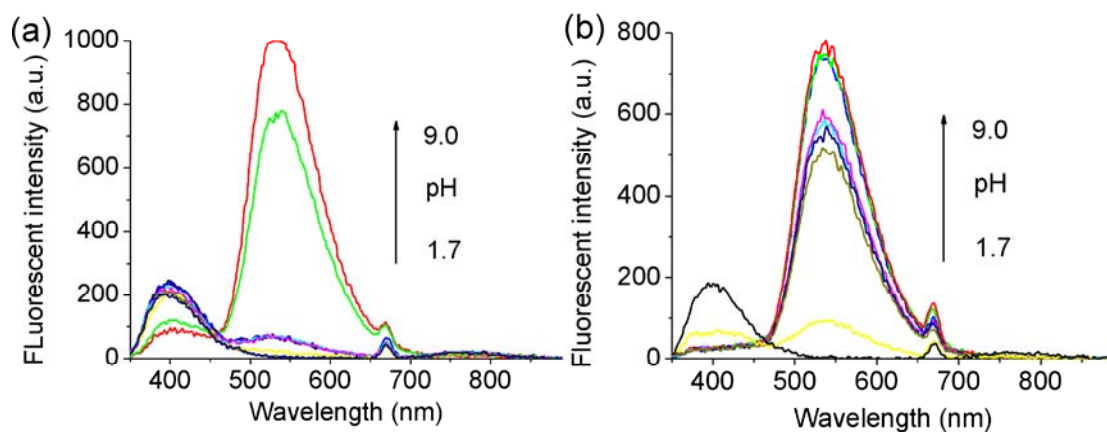


**Fig. S10.** (a) Fluorescence spectra of sensor **1** and (b) sensor **1** + 2.0 equiv F<sup>-</sup> at various pH values in DMF/H<sub>2</sub>O (95:5, v/v). [**1**] = 200 μM. λ<sub>ex</sub> = 335 nm.

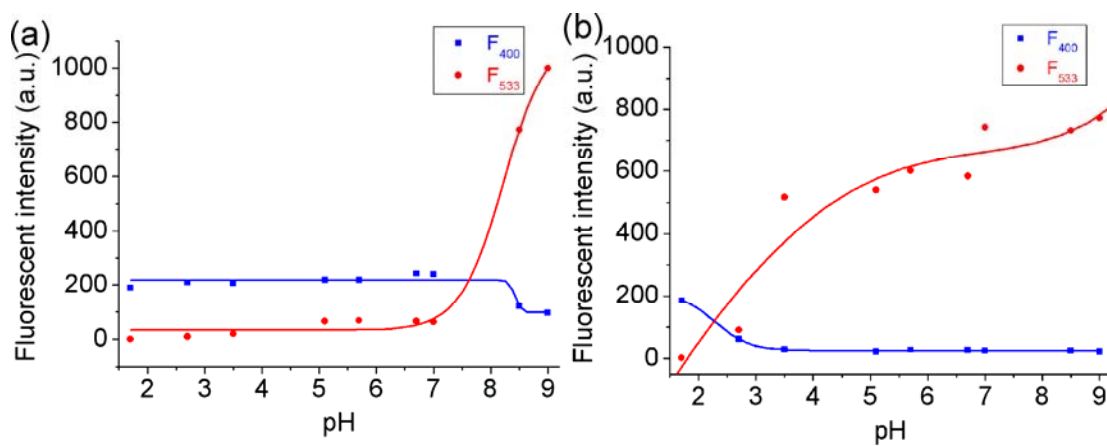


**Fig. S11.** (a) Fluorescence intensity of **1** and (b) sensor **1** + 2.0 equiv F<sup>-</sup> at 400 nm and 533 nm recorded at various pH values in DMF/H<sub>2</sub>O (95:5, v/v). [**1**] = 200 μM. λ<sub>ex</sub> = 335 nm.

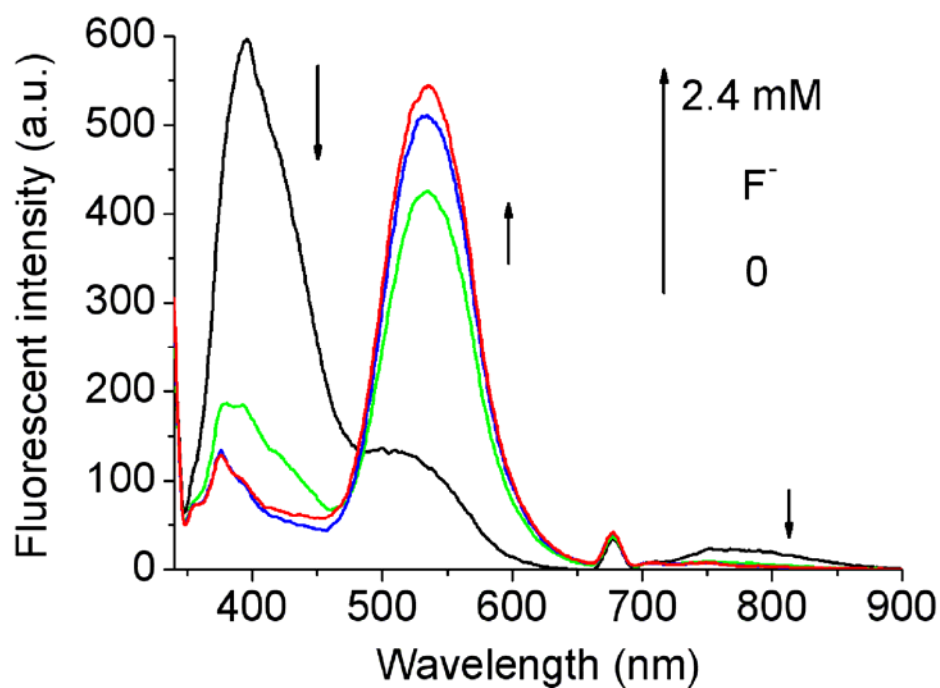


**Fig. S12.** (a) Fluorescence spectra of sensor **1** + TBAF in DMF/H<sub>2</sub>O (90:10, v/v) in the presence of increasing F<sup>-</sup> concentrations. [1] = 200 μM. λ<sub>ex</sub> = 335 nm.

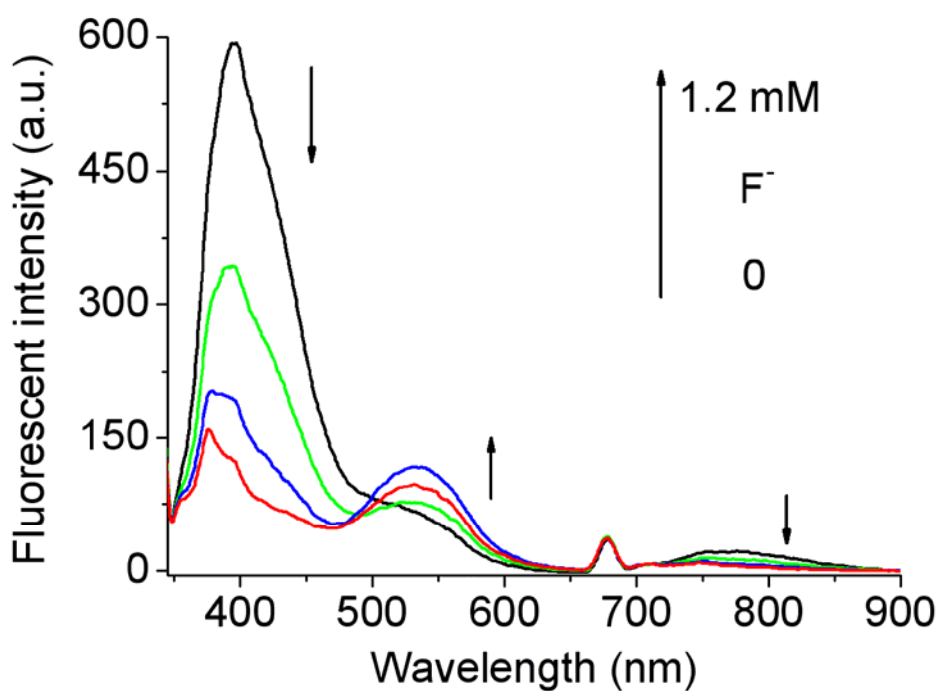


**Fig. S13.** (a) Fluorescence spectra of sensor **1** + TBAF in DMF/H<sub>2</sub>O (80:20, v/v) in the presence of increasing F<sup>-</sup> concentrations. [1] = 200 μM. λ<sub>ex</sub> = 335 nm.

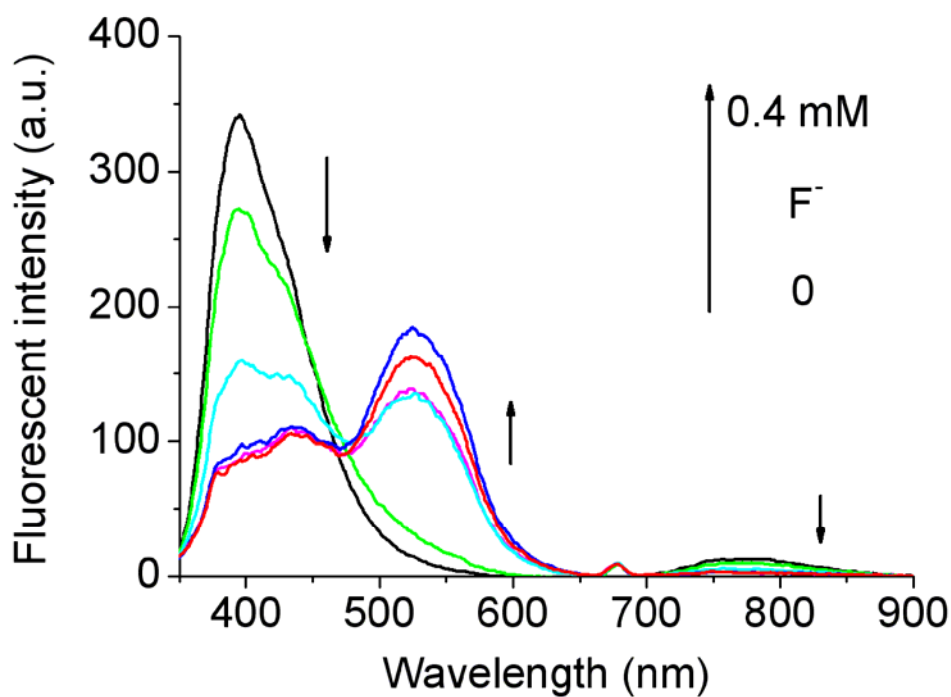


**Fig. S14.** (a) Fluorescence spectra of sensor **1** + TBAF in THF/H<sub>2</sub>O (95:5, v/v) in the presence of increasing F<sup>-</sup> concentrations. [1] = 200 μM. λ<sub>ex</sub> = 338 nm.

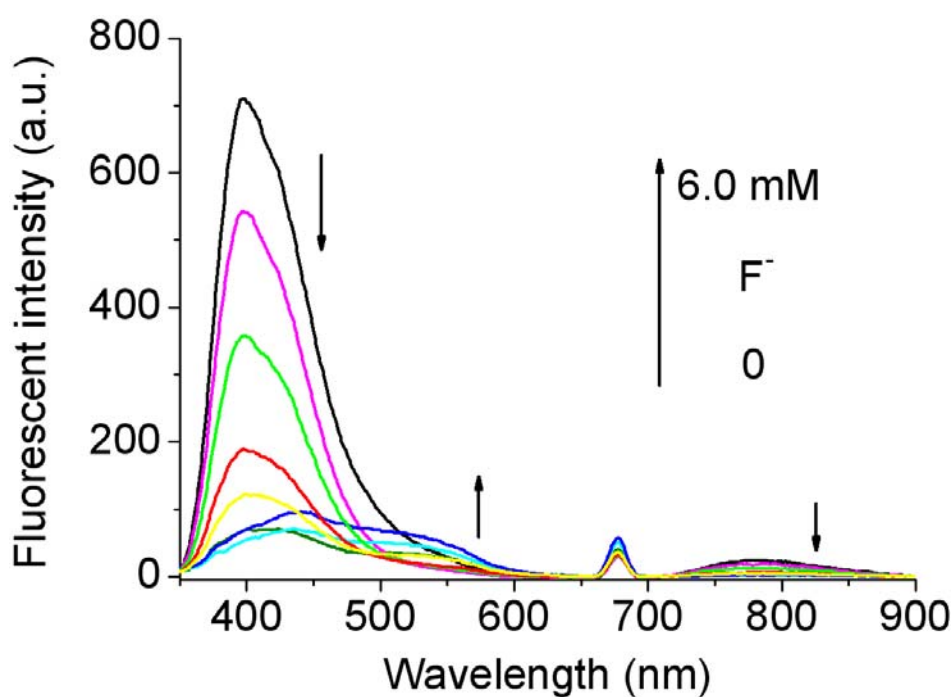


**Fig. S15.** (a) Fluorescence spectra of sensor **1** + TBAF in CH<sub>3</sub>CN/H<sub>2</sub>O (95:5, v/v) in the presence of increasing F<sup>-</sup> concentrations. [1] = 200 μM. λ<sub>ex</sub> = 335 nm.

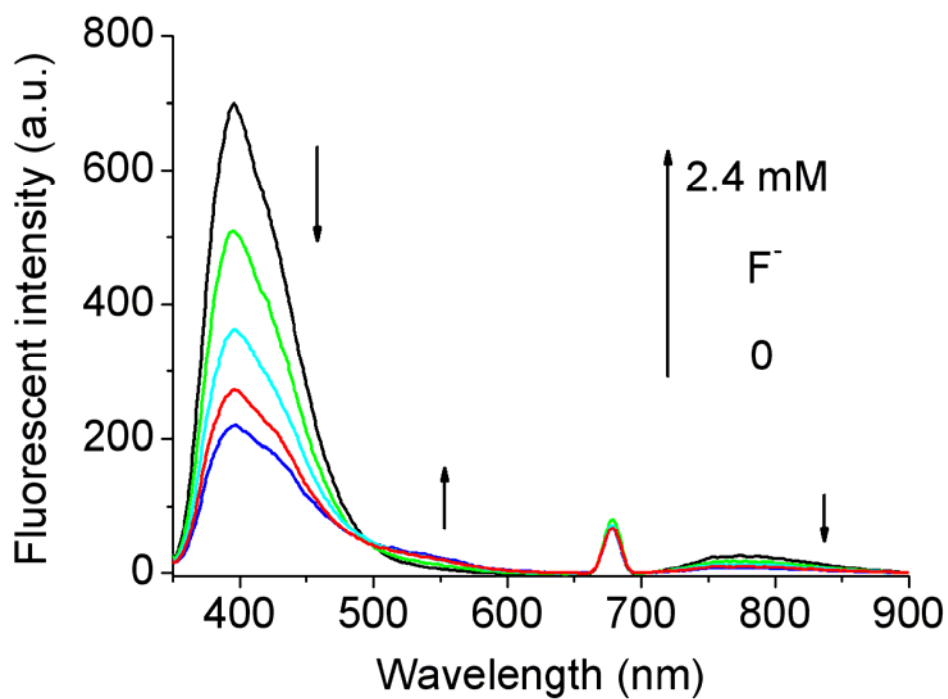


**Fig. S16.** (a) Fluorescence spectra of sensor **1** + TBAF in dioxane/H<sub>2</sub>O (95:5, v/v) in the presence of increasing F<sup>-</sup> concentrations. [1] = 200 μM. λ<sub>ex</sub> = 335 nm.

## 5. <sup>1</sup>H NMR Analysis

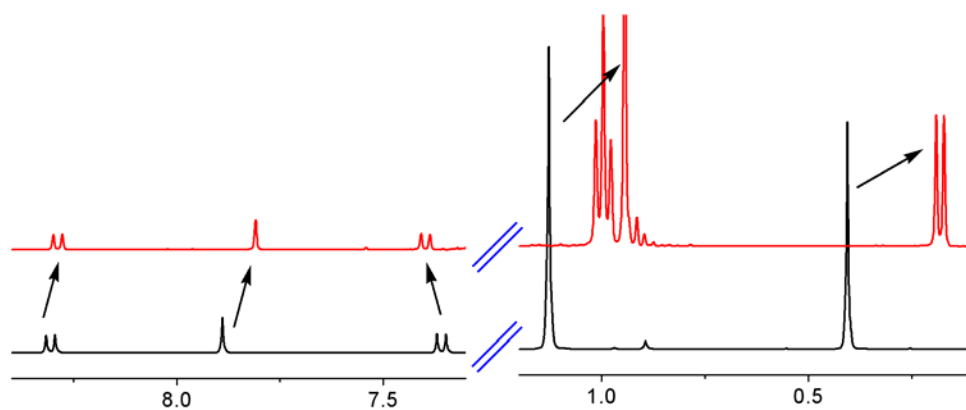


**Fig. S17.** <sup>1</sup>H NMR spectrum of **1** (bottom) and **1**+1.0 equivalent F<sup>-</sup> (top) taken in CDCl<sub>3</sub>.

## 6. NMR and MS Data.

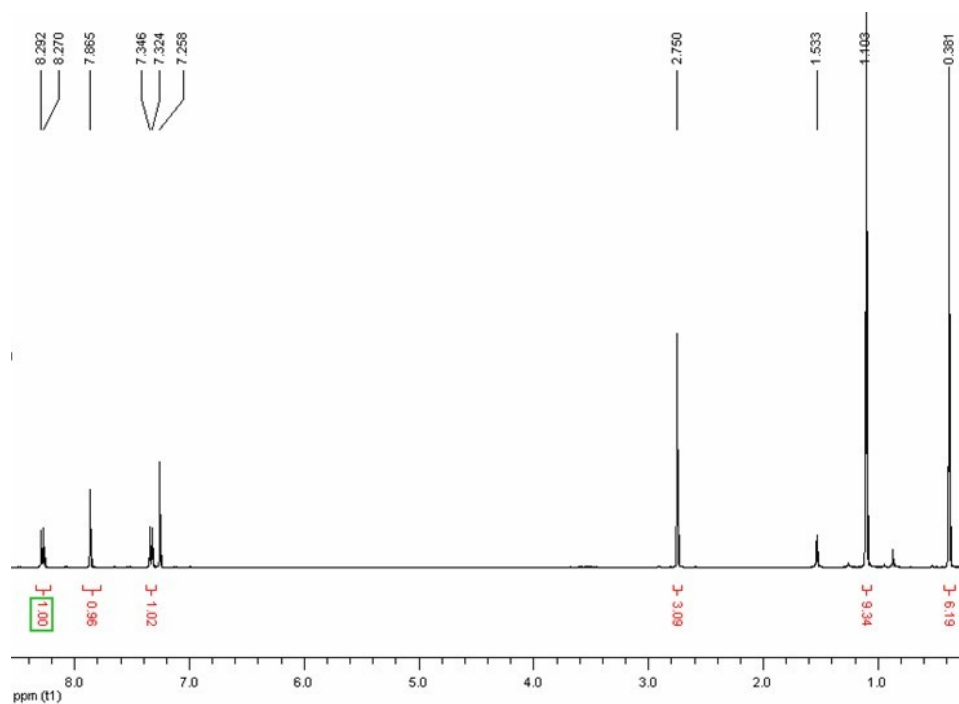


**Fig. S18.**  $^1\text{H}$  NMR ( $\text{CDCl}_3$ , 400 MHz) spectrum of **1**.

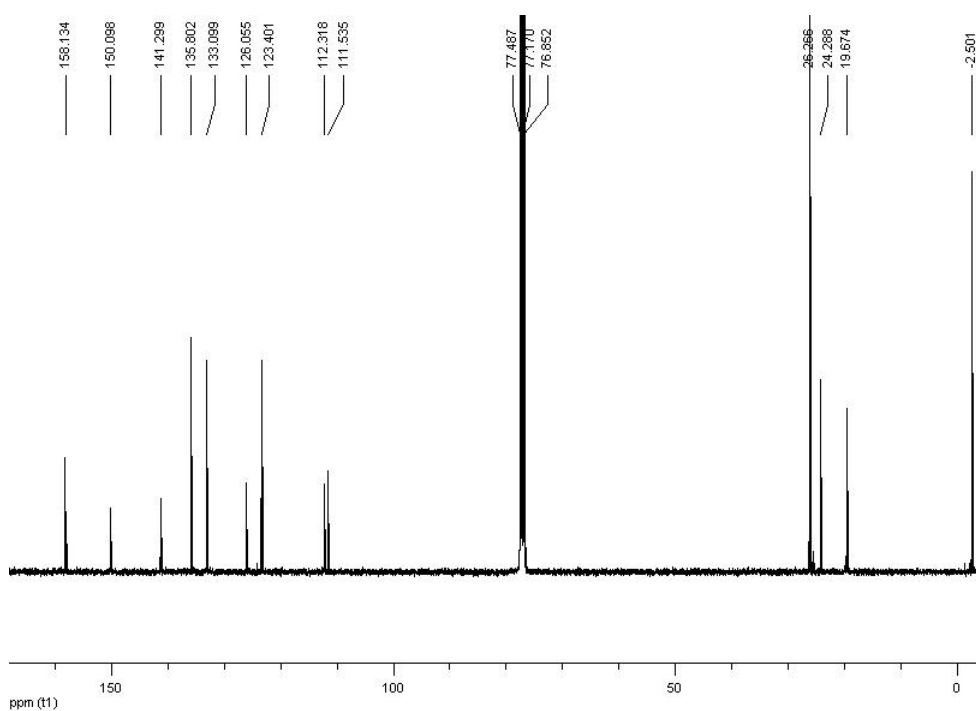


**Fig. S19.**  $^{13}\text{C}$  NMR ( $\text{CDCl}_3$ , 400 MHz) spectrum of **1**.

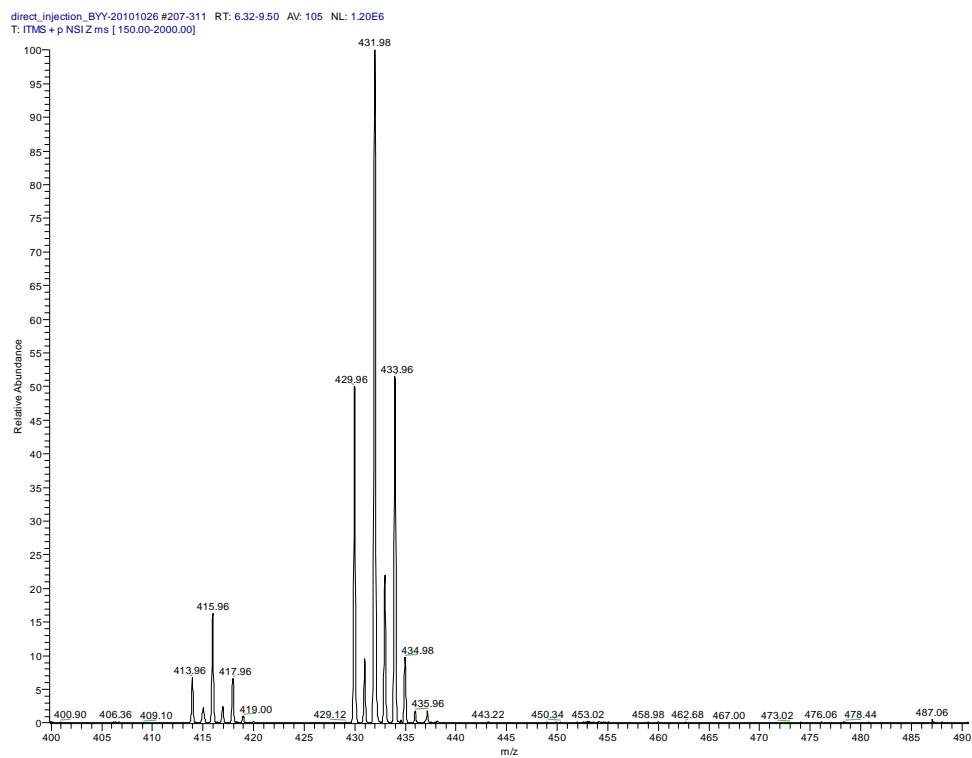


**Fig. S20.** Mass spectrum of **1**.

## References

1. N. Jotterand, D. A. Pearce, and B. Imperiali, *J. Org. Chem.* 2001, 66, 3224.
2. Olmsted, J. *J. Phys. Chem.* **1979**, 83, 2581.